Journal of Alloys and Compounds 504S (2010) S418–S421

Contents lists available at ScienceDirect

Journal of Alloys and Compounds

journal homepage: www.elsevier.com/locate/jallcom

Effects of film density on electrochromic tungsten oxide thin films deposited by reactive dc-pulsed magnetron sputtering

Xilian Sun*, Zhimin Liu, Hongtao Cao

Division of Functional Materials and Nano Devices, Ningbo Institute of Material of Technology & Engineering, Chinese Academy Sciences, Ningbo 315201, PR China

ARTICLE INFO

Article history:
Received 15 June 2009
Received in revised form 16 March 2010
Accepted 18 March 2010
Available online 25 March 2010

Keywords:
Tungsten oxide film
Electrochromic
Film density
Reactive sputtering

ABSTRACT

The correlation between the electrochromic performance and the film density of the tungsten oxide thin films sputtered by reactive dc-pulsed magnetron sputtering with varying working pressure was investigated. It is found that the optical modulation and coloration efficiency of films are strongly affected by the amount of tungsten oxide present in the film. The coloration kinetic is also found to be sensitive to the film density, with the maximum value of 3.48×10^{-10} cm^2/s for the porous film deposited at higher pressure. X-ray diffraction and TEM showed that the films were amorphous. By using spectroscopic ellipsometer to anaylsis the surface roughness and refractive index of the sputtered films, we found that the film at higher working pressure was rough and lower density, which offered fast electrochromic response.

1. Introduction

Electrochromic materials have attracted considerable attention due to their application in smart window, displays and variable reflectance mirrors [1–4]. Tungsten oxide has been extensively studied as a promising electrochromic material for its high coloration efficiency and better electrochemical stability as compared with other electrochromic materials [5–7]. When electrons and ions are injected or extracted under an applied electric field, the electronic structure of WO_3 is modified, namely, the Fermi level is moved upwards. Thus, the excess electrons fill the t_{2g} band of perovskite WO_3 and the optical property of WO_3 transforms from a transparent state to an absorbing one. So for electrochromic materials electronic conductivity and ionic diffusivity are critical factors. It is known that the kinetics of propagation of polarons (e^-, M^+) is mainly limited by cation diffusion in the inorganic matrix, which is strongly dependent on the overall material morphology, microstructure and crystallinity [8,9]. The commonly employed deposition techniques are thermal evaporation, electron beam evaporation, sputtering, pulsed laser ablation, chemical vapor deposition, sol–gel coating and electrodeposition. DC reactive magnetron sputtering is well established process for the deposition of compound films, which has been largely used [10,11]. But the main drawback is that the target and the walls of the deposition chamber are covered by randomly grown insulating layers, resulting in microarcs and target poisoning. The pulse technique may eliminate the random arcing phenomena by supplying the DC power in the form of high negative pulses interrupted by small positive pulses. In this way the charge at the oxide surface on the target may be neutralized by attracting electrons during the positive part of the duty cycle [12]. This technique can preserve high deposition rates contrary to the RF techniques. This paper focuses on the deposition of tungsten oxide by pulsed dc magnetron sputtering in an argon and oxygen gas mixture. The simplest and most important parameter in a sputter process is total pressure. In this study the correlation between the film properties, e.g. microstructural and electrochromic properties, and total pressure has been investigated.

2. Experimental procedures

2.1. Sample preparation

The tungsten oxide thin films were deposited onto SnO_2:F (FTO) coated glass (14 Ω/□, 10 mm × 20 mm) and Si wafer from W metal target (99.99% purity, 2-in. in diameter) at room temperature by pulsed dc magnetron sputtering in an argon and oxygen plasma. The sputtering chamber was evacuated to 2.6×10^{-4} Pa using a turbo molecular pump and a dry pump before introducing gases. The gas pressure was maintained by mass-flow controllers via a gas inlet. The target was sputtered for 10 min before starting the deposition to clean the surface of any oxide layer. The dc power was 100 W. The pulse frequency was 20 kHz and the reverse time was 5 μs. The gas composition was adjusted by two mass-flow controllers with a constant Ar/O_2 ratio of 4 and the resulting total pressure, P, was varied from 0.41 to 1.7 Pa. In this range, the discharge voltage moved from 357 to 353 V and the current changed from 0.277 to 0.282 A. For convenience, three samples was labeled as S1, S2, S3, S4 and S5 corresponding to the chamber pressure of 0.41, 0.65, 0.89, 1.3 and 1.7 Pa, respectively.

* Corresponding author. Tel.: +86 0574 86685163; fax: +86 0574 86685163.
E-mail address: xiliansun@163.com (X. Sun).

0925-8388/$ – see front matter © 2010 Elsevier B.V. All rights reserved.
doi:10.1016/j.jallcom.2010.03.155

Table 1
Thickness, deposition rate, refractive index, relative density and band gap energies (E_g) of the reactive dc-pulsed sputtering tungsten oxide films as a function of working pressure.

Samples	Working pressure (Pa)	d (nm)	Deposition rate (nm min^{-1})	E_g (eV)	n at 550 nm	Relative density at 550 nm
S1	0.41	140	4	3.31	2.18	0.90
S2	0.65	135	3.1	3.32	2.05	0.85
S3	0.89	135	2.5	3.37	1.99	0.82
S4	1.3	120	1.5	3.38	1.98	0.81
S5	1.7	121	1.1	3.43	1.97	0.81

2.2. Characterization

Film thickness and refractive index, n, were measured on Si substrates by a variable angle spectroscopic ellipsometer (Woollam M-2000, USA). Optical properties were measured with an ultraviolet-visible-infrared spectrophotometer in the wavelength region of 300–2000 nm. X-ray diffraction (XRD) patterns of the virgin films were recorded in the 2θ range from 20° to 70° with a Bruker AXS D8 advance diffractometer, using Cu $K\alpha$ radiation. The electrochromic properties were characterized using cyclic voltammetry method between −1 and +1 V at a scan rate of 20 mV/s. A standard three-electrode configuration consisting of the sample as the working electrode, a Pt counter electrode and a conventional saturated Ag/AgCl as the reference electrode, was used to perform the electrochemical tests. The electrolyte was a 1.0 M $LiClO_4$ propylene carbonate solution.

3. Results and discussions

3.1. Characteristics of tungsten oxide films

The effect of total pressure on the deposition rate of films has been investigated and summarized in Table 1. The results confirm that the deposition rate increases with decreasing total pressure, as expected from an enhanced mean free path of plasma species. The mean free path of the atoms in a gas is given by [13]:

$$\lambda = \frac{2.33 \times 10^{-20} T}{P\delta_m^2}$$

where T is the temperature, P is the pressure and δ_m is the atomic (or molecular) diameter of the sputtering gas. Thus, as the pressure decreases the mean free path of the gas atoms increases, and hence the collision frequency decreases.

X-ray diffraction patterns of tungsten oxide films at different total pressure are shown in Fig. 1. XRD peaks come from the FTO layer of K-glass substrate, without sharp peaks of samples being found. It indicates that the film is of poor crystallinity. Transmission electron microscopy (TEM) and selected area electronic diffraction (SEAD) pattern of the film shows some halo rings, which further confirms the amorphous nature. The amorphous diffraction pattern may result from the amorphous property and internal stress of tungsten oxide films, which is usually a property of films prepared by sputter-deposition at room temperature [14].

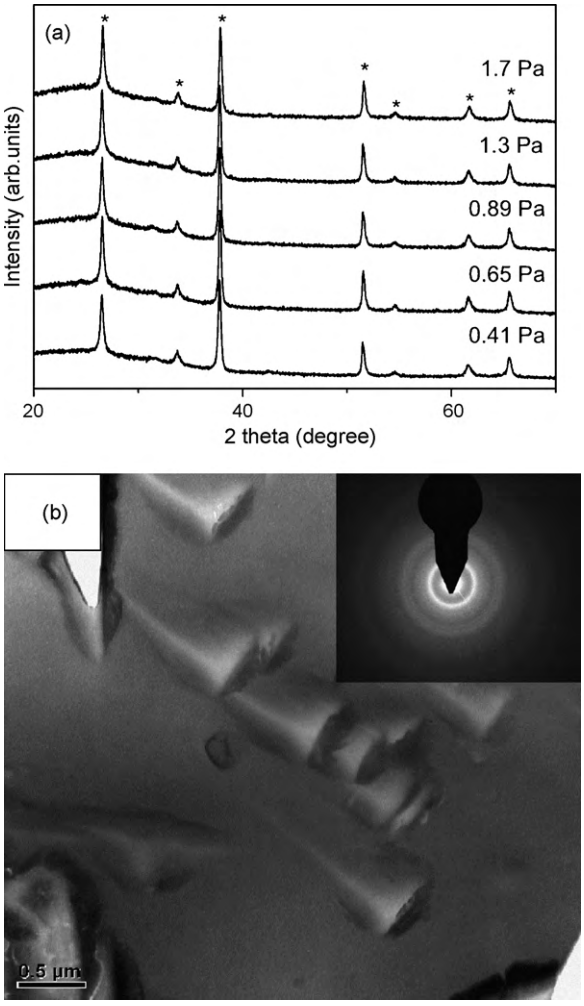

Fig. 1. (a) X-ray diffraction patterns of tungsten oxide films deposited at different total pressure. *FTO peaks. (b) TEM image and SAED pattern (inset) of tungsten oxide films.

3.2. Optical properties

Fig. 2 shows the refractive index of tungsten oxide films dependence on total pressure. As can been seen, the refractive index of WO_3 films decreases when the total pressure increases. The significant increase in the refractive index of the films with decreasing working pressure confirms the enhancement of the packing density. The relative density is defined as the ratio of the densities of the film to that of the bulk. The Lorentz–Lorentz relationship for the relative density P, is given by [15]

$$P = \left(\frac{\rho_f}{\rho_b}\right) = \left(\frac{n_f^2 - 1}{n_f^2 + 1}\right)\left(\frac{n_b^2 + 1}{n_b^2 - 1}\right)$$

where ρ is the density and n is the refractive index at 550 nm; the subscripts f and b refer to the film and the bulk, respectively. The bulk refractive index of WO_3 at 550 nm is 2.5 [16]. The results are

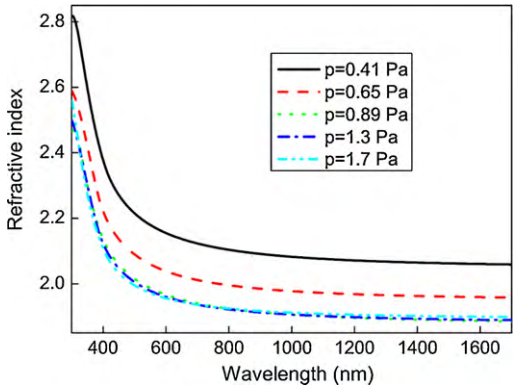

Fig. 2. Refractive index of tungsten oxide films dependence on total pressure.

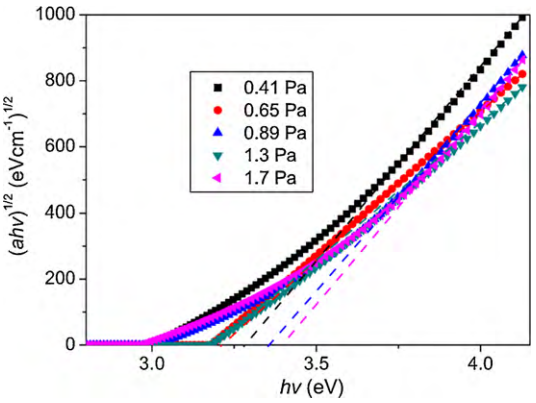

Fig. 3. Absorption spectra plotted as $(\alpha h\nu)^{1/2}$ vs. photo energy ($h\nu$) for tungsten oxide films.

summarized in Table 1. One can immediately observe the high-pressure deposited film is much less dense than the low-pressure samples.

The optical band gap (E_g) was evaluated from the absorption coefficient (α) using the relationship for indirect allowed transitions: $(\alpha h\nu)^{1/2} = A(h\nu - E_g)$, where A, $h\nu$ and E_g are a constant of proportionality, incident photon energy and optical band gap energy, respectively. The absorption coefficient (α) is obtained by the following expression: $\alpha(\lambda) = (1/d)\log[(1 - R(\lambda))/T(\lambda)]$, where d denotes the thickness of the film. The plots of $(\alpha h\nu)^{1/2}$ vs. $h\nu$ for all the films is illustrated in Fig. 3. The optical band gap of the films estimated by this method was found to be 3.31, 3.32, 3.37, 3.38 and 3.43 eV for the samples S1, S2, S3, S4 and S5, respectively. Since the band gap of bulk WO_3 is reported to be 2.62 eV for indirect transitions [17], the larger band gaps observed are possibly due to amorphous nature of the WO_3 films. Further, the dependence of band gap on the pressure is systematic: the band gap initially increases from 3.31 for S1 to 3.37 for S3, then it increases to 3.43 for S5 samples. Following the earlier report that the denser films show lower band gap than the porous ones [18], the present observation may be attributed to the difference in the density of the films.

3.3. Electrochromic properties

The films were colored using a potential of −1 V for 20 s in order to determine their ion storage capacities, optical modulation (ΔT) and coloration efficiency (CE). The dependence of optical transmittance modulation and coloration efficiency on the wavelength ranging from 300 to 2000 nm for the WO_3 films is illustrated in Fig. 4. The optical modulation of the WO_3 films is observed to decrease with increasing total pressure and exhibits the largest modulation of visible radiation (Fig. 4a). The change in the optical modulation and the amount of intercalated charge bring about a corresponding change in coloration efficiency (CE(λ)) (Fig. 4b), and is given by the following relation: $CE(\lambda) = \ln(T_b/T_c)/(Q/A)$, where T_b and T_c are the transmissions in the bleached and the colored states of the WO_3 film, Q is the amount of charge intercalated and A is the area of the colored film. It was found that the coloration efficiencies for the films increase with increasing density of the film, in other words, the coloration efficiency is strongly correlated with the amount of tungsten oxide present in the films. One of the physical properties of the film that significantly influence the intercalating charge is the film density. A porous film is expected to enhance the ion conductivity as well as provide a large interface

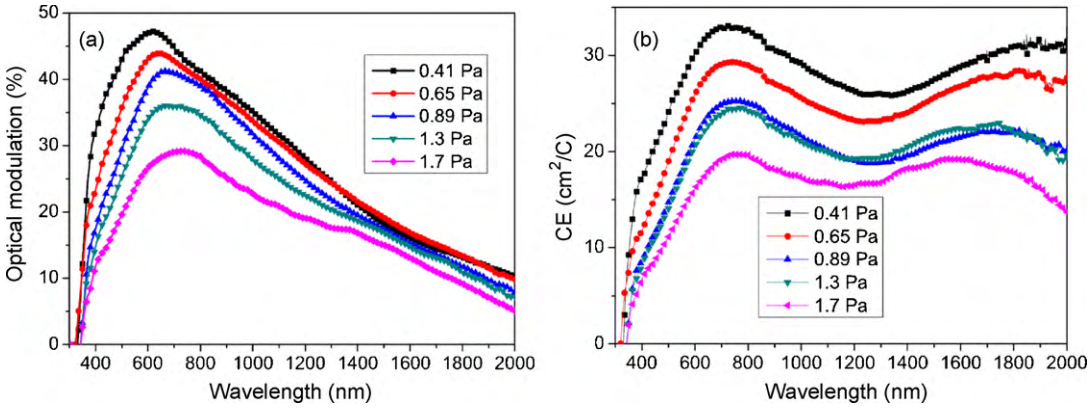

Fig. 4. Optical modulation (a) and coloration efficiency (b) of WO_3 thin films with different total pressure.

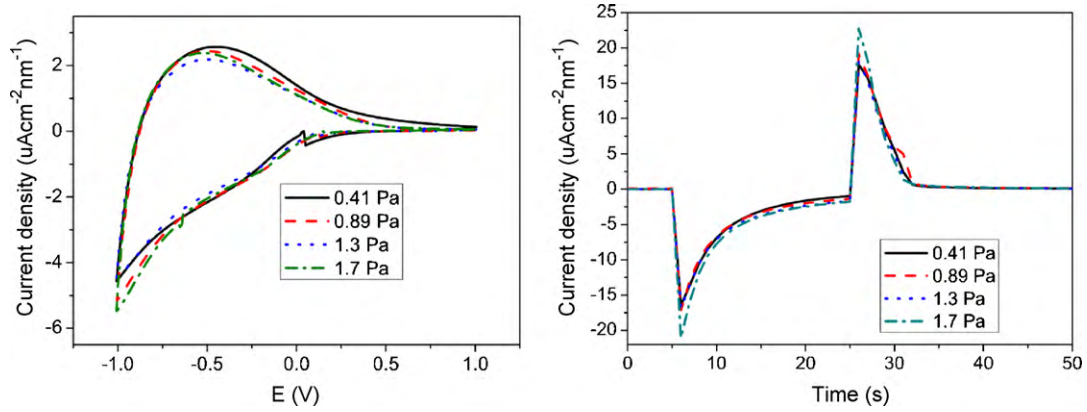

Fig. 5. Cyclic voltammograms and chronoamperometry of WO_3 films deposited at different total pressure.

Table 2
Charge storage capacity, anodic peak current and diffusion coefficient of WO_3 films.

Samples	Ion storage capacity ($\mu C/cm^2$ nm)	Anodic peak current, i_{pa} ($\mu A/cm^2$ nm)	Diffusion coefficient, D ($\times 10^{-10}$ cm^2/s)	Reversibility
S1	252.2	15.4	1.60	0.51
S2	261.4	16.9	1.95	0.52
S3	283.8	17.9	2.16	0.60
S4	296.2	19.3	2.51	0.64
S5	371.6	22.7	3.48	0.72

for lithium ion insertion, thus improving the speed of coloration and coloration efficiency with the same amount of inserted charge as a consequence of high number of available sites. However, the porous films in the present study exhibit lower optical modulation and coloration efficiency. Azimirad et al. [19] reports that the CE of WO_3 films vary linearly with thickness. From the above results we could conclude that the high coloration efficiency for amorphous film obtained with the same amount of inserted charge is a consequence of high number of available sites.

Typical cyclic voltammograms (CVs) recorded at a scan speeds of 20 mV/s for the WO_3 films are displayed in Fig. 5a. All of the CVs were normalized to the geometric area of the electrode and to the thickness of tungsten oxide film, resulting in units of $\mu A\,cm^{-2}\,nm^{-1}$. The current recorded is due to a cation intercalation/deintercalation according to the reaction:

$$WO_3(\text{bleach}) + xLi^+ + xe^- \leftrightarrow Li_xWO_3(\text{blue})$$

where Li^+ is ion in lithium perchlorate organic solution. The integrated cathodic-current density equates to the amount of lithium ions intercalated to form a tungsten bronze. When compared with the cathodic charge quantities of samples deposited at higher pressure, the S5 samples show a higher charge-insertion density over the same time period, indicating faster kinetics. It is possible to evaluate the diffusion coefficient of the ions from the CV curves. The diffusion coefficient for the ion from the peak anodic current may be calculated using Randles–Servicik equation [20]:

$$i_p = 2.72 \times 10^5 \times n^{3/2} \times D^{1/2} \times c_0 \times v^{1/2}$$

where i_p is the peak anodic current (mA), $n = 1$ is the number of electrons involved in the process, D ($cm^2\,s^{-1}$) is the diffusion coefficient, C_0 is the solution concentration ($mol\,cm^{-3}$) and v is the scan rate ($V\,s^{-1}$). The results are summarized in Table 2. It clearly shows that the diffusion coefficient increases as the working pressure increases. The charges inserted for the sample deposited at higher pressure during intercalation process is always greater than that deposited at lower pressure. The CV area increases as total pressure increases. The improved lithium-insertion ability of the S1 sample is attributed to its low density and high active suface area, compared with the other four samples. Note also that the onset of a cathodic current for S5 sample is more positive compared with the other samples. This early onset of a cathodic current for S5 films may indicate reduced interfacial charge-transfer resistance, providing another reason for the improved electrochemical response.

Fig. 5b shows the chronoamperometry (CA) data of the tungsten oxide thin films with the potential being stepped from −1 to +1 V for 20 s. The plots indicate a faster decay in the currents in the case of porous film when compared to the dense film, both during coloration and bleaching. This suggests that bleaching and coloration kinetics are faster for S5 film than the other two denser films as a lower film density corresponds to a more porous film which allows faster ion incorporation and hence results in a faster coloration-bleaching kinetics behavior. The reversibility of the films calculated as the ratio of charge deintercalated (Q_{ex}) to charge intercalated (Q_{in}) in the film. It was observed that the reversibility increases as the film density increases and found maximum of for S5.

4. Conclusion

The tungsten oxide thin films were deposited by reactive dc-pulsed sputtering technology at different working pressure. The effects of working pressure on the optical and electrochromic properties of the films are discussed. The as-deposited films are amorphous. The films deposited at higher total pressure exhibit a lower density which allows for easy transport of ions across the film and thus enhances the coloration dynamics. And they are optically reversible and show the smallest coloration and bleaching times. Furthermore, the electrochromic properties of tungsten oxide films are strongly correlated with film density as well as thickness. From electrochromic device functionality viewpoint, both the coloration efficiency and the speed of coloration are important. This study indicates that the film with lower density and larger thickness is desirable for better electrochromic properties.

Acknowledgment

The authors gratefully acknowledge the financial support provided by Science and Technology Department of Zhejiang Province of China (2008C31G3220006).

References

[1] C.-C. Liao, F.-R. Chen, J.-J. Kai, Solar Energy Mater. Solar Cells 91 (2007) 1282.
[2] D.R. Rosseinsky, R.J. Mortimer, Adv. Mater. 13 (2001) 783.
[3] N.A. O'Brien, J. Gordon, H. Mathew, B.P. Hichwa, Thin Solid Films 312 (1999) 345.
[4] G.A. Niklasson, C.G. Granqvist, J. Mater. Chem. 17 (2007) 127.
[5] C.G. Granqvist, Solar Energy Mater. Solar Cells 60 (2000) 201.
[6] J. Livage, D. Ganguli, Solar Energy Mater. Solar Cells 68 (2001) 365.
[7] A. Patra, K. Auddy, D. Ganguli, J. Livage, P.K. Biswas, Mater. Lett. 58 (2004) 1059.
[8] P. Judeinstein, J. Livage, J. Chem. Phys. 90 (1993) 1137.
[9] T. Brezesinski, D.F. Rohlfing, S. Sallard, M. Antonietti, B.M. Smarsly, Small 2 (2006) 1203.
[10] C.G. Granqvist, Handbook of Inorganic Electrochromic Materials, Elsevier, Amsterdam, 1995.
[11] C. Brigouleix, P. Topart, E. Bruneton, F. Sabary, G. Nouhaut, G. Campet, Electrochim. Acta 46 (2001) 1931.
[12] L.B. Jonsson, T. Nyberg, I. Katardjiev, S. Berg, Thin Solid Films 365 (2000) 43.
[13] L.I. Maissel, R. Glang, Handbook of Thin Film Technology, McGraw-Hill, New York, 1970, p. 1.
[14] X.G. Wang, Y.S. Jiang, N.H. Yang, L. Yuan, S.J. Pang, Appl. Surf. Sci. 143 (1999) 135.
[15] E. Washizu, A. Yamamoto, Y. Abe, M. Kawamura, K. Sasaki, Solid State Ionics 165 (2003) 175.
[16] S. Sawada, G.C. Danielson, Phys. Rev. 113 (1959) 1008.
[17] F.P. Koffyberg, K. Dwight, A. Wold, Solid State Commun. 30 (1979) 433.
[18] A. Subrahmanyam, A. Karuppasamy, Solar Energy Mater. Solar Cells 91 (2007) 266.
[19] R. Azimirad, O. Akhavan, A.Z. Moshfegh, J. Electrochem. Soc. 153 (2006) E11.
[20] M. Deepa, R. Sharma, A. Basu, S.A. Agnihotry, Electrochim. Acta 50 (2005) 3545.